Residual ultimate strength of damaged seamless metallic pipelines with metal loss

Cai, Jie; Jiang, Xiaoli; Lodewijks, Gabriel; Pei, Zhiyong; Wu, Weiguo

DOI
10.1016/j.marstruc.2017.11.011

Publication date
2018

Document Version
Final published version

Published in
Marine Structures

Marine Structures 58 (2018) 242–253

Contents lists available at ScienceDirect

Marine Structures

journal homepage: www.elsevier.com/locate/marstruc

Residual ultimate strength of damaged seamless metallic pipelines with metal loss

Jie Cai[a,*], Xiaoli Jiang[a], Gabriel Lodewijks[b], Zhiyong Pei[c], Weiguo Wu[c]

[a] Department of Maritime and Transport Technology, Delft University of Technology, 2628 CD Delft, The Netherlands
[b] School of Aviation, University of New South Wales, NSW 2052, Sydney, Australia
[c] Departments of Naval Architecture, Ocean and Structural Engineering, School of Transportation, Wuhan University of Technology, PR China

ARTICLE INFO

Keywords:
Metallic pipelines
Metal loss
Residual ultimate strength
Nonlinear FEM
Pipe tests

ABSTRACT

On the basis of an experimental investigation [1], numerical investigation is conducted in this paper on damaged seamless metallic pipelines with metal loss (diameter-to-thickness ratio D/t around 21) through nonlinear finite element method (FEM). Numerical models are developed and validated through test results by using the measured material properties and specimen geometry, capable of predicting the residual ultimate strength of pipes in terms of bending capacity (M_{cr}) and critical curvature (κ_{cr}). By changing the metal loss parameters, i.e. length (l_m), width (w_m) and depth (d_m), a series of numerical simulations are carried out. Results show that the larger the d_m or l_m is, the less the bending capacity will be. The increase of notch width slightly reduces the pipe strength, presenting a linear tendency. Based on the FEM results, empirical formulas are proposed to predict the residual ultimate strength of metallic pipes with metal loss under pure bending moment. The prediction results match well with the results from the tests, the numerical simulations as well as the theoretical derivation. Such formulas can be therefore used for practice purposes and facilitate the decision-making of pipe maintenance after mechanical interference.

1. Introduction

In previous work [1], an extensive experimental investigation on the structural behavior of damaged seamless metallic pipelines (D/t around 21) subjected to bending moment has been completed. The specimens deployed had an average outer diameter (D) of 168.3 mm and an average thickness (t) of 8 mm. Artificial structural damage was imposed on the surface of specimens including a dent, metal loss in the form of notch, crack and combinations thereof. For intact pipelines, the elastic-plastic failure mode dominates. The structures fail smoothly, initiated in the form of an outward bulge in the area away from the specimen central cross-section. However, the failure of damaged specimens with either a dent or a notch has been accelerated due to the rapid localization of damaged area, with a decrease of both bending capacity and corresponding critical curvature. As one of the numerical investigation series, the present research only concentrates on damaged pipes with metal loss in terms of a notch in order to quantify its effect.

Metal loss is a generalized type of damage that involves partial loss of material in the forms of gouges and notches, etc. In pipelines, metal loss defects due to mechanical interference may compromise structural safety and lead to large loss of assets [2]. Unlike the widely investigation of corrosion on metallic pipes [3–5], the investigation of such metal loss is relative rare due to low probability of mechanical interference. It has been estimated that the failure of oil and gas transmission pipelines that was resulted from structural damage ranges from 55% in the US to around 70% in Europe [6]. Scenarios in practice such as dropping of foreign

* Corresponding author.
E-mail address: J.Cai-2@tudelft.nl (J. Cai).

https://doi.org/10.1016/j.marstruc.2017.11.011
Received 18 August 2017; Received in revised form 27 October 2017; Accepted 26 November 2017
Available online 06 December 2017
0951-8339/

Nomenclature

κ_0	referential curvature of pipe [1/m]
κ_i	critical curvature of intact pipe (either from test or simulation) [1/m]
κ_{cr}	critical curvature of damaged pipe [1/m]
λ_l	normalized notch length
λ_w	normalized notch width
ϕ	half angle of metal loss [radians]
σ_y	material yield strength [MPa]
σ_{comp}	compression stress in pipe cross-section [MPa]
σ_{ten}	tensile stress in pipe cross-section [MPa]
θ	angle from bending plane to the plastic neutral axis [radians]
D	outer diameter of pipe [mm]
d_m	metal loss depth [mm]
F	true axial force [N]
k_1, k_2	constants related to notch depth
L_0	length of pipe under pure bending [mm]
l_m	metal loss length [mm]
M_i	ultimate bending moment of intact pipe (either from test or simulation) [kNm]
M_y	plastic bending moment [kNm]
M_{cr}	residual ultimate bending moment [kNm]
R	pipe outer radius [mm]
R_a	pipe average radius [mm]
R_m	reduced average pipe radius due to notch, expressed as $R_m = R_a - d_m/2$
S_m	compression area of metal loss region
S_{comp1}	compression area of region without metal loss
S_{loss}	area loss of metal loss in pipe cross-section
S_{ten}	tensile area of pipe cross-section
t	pipe thickness [mm]
t_m	reduced pipe thickness due to notch, expressed as $t_m = t - d_m$
w_m	metal loss width [mm]
Y_m, Y_{comp1}, Y_{ten}	force arms from bending axis to the mass center of respective area segment

objects, fishing equipment, dragging anchors and sinking vessels [7–9] can introduce considerable metal loss on pipes so that the residual ultimate strength of structure may be affected. In this paper, a notch is used to represent such metal loss on the outer surface of metallic pipes.

Considerable research on the ultimate strength behavior of pipes subjected to bending moment has been conducted in the past few decades. In the early time, Bai et al. [10] proposed prediction equations on the ultimate limit states of intact pipes with D/t ratios from 10 to 40 based on an existing experimental database. Experimentally, Es et al. [11] investigated ultimate strength of pipes without structural damage subjected to bending moment, deploying a spiral-welded steel tubes with 42-inch-diameter and D/t between 65 and 120. Based on the test results, Vasilikis et al. [12] conducted a consecutive numerical investigation. Other relevant research can be also seen from literature [13–18].

Nevertheless, most of the investigations focused on ultimate strength of intact metallic pipes. The investigations on pipes with metal loss under bending moment are relatively rare. Levold et al. [19] conducted a test on a damaged pipe with D/t of 26.5, where corrosion damage in terms of gouge was artificially introduced in the inner surface of pipe by Electrical Discharge Machining (EDM) method. In addition, the so-called “neighbor response” effect of finite metal loss has not been fully taken into account in most of the existed research. Zheng et al. [20] used the “effective thickness” to correct such effect. Other investigation on damaged pipes mainly concentrates on the busting of pipes subjected to internal pressure or the collapse capacity of pipes subjected to external pressure, such as Park and Kyriakides [21] and Bjrny et al. [7].

Therefore, the objective of this paper is to investigate the structural behavior of seamless metallic pipes with notch on the compression side and quantify the damage effect. The structure of this paper is arranged as follows. In Section 2, the four-point bending test set-up and the specimens deployed in this research are briefly reviewed. Section 3 comprehensively describes the developed numerical models for simulation of pipes with metal loss. Furthermore, the numerical model is validated through test in terms of failure mode, bending moment-curvature diagrams and ultimate strength in Section 4. In Section 5, the simulation results of notch are investigated and discussed. Analytical solution of residual bending moment accounting for the changing of neutral axis due

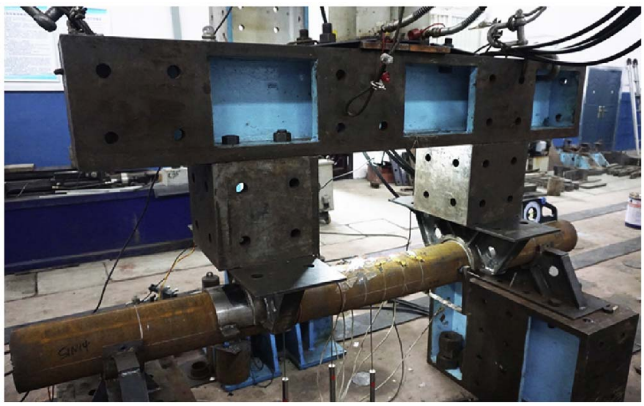

Fig. 1. The configuration of four-point bending test set-up in laboratory [1].

to damage is carefully derived. Empirical formulas are then proposed to predict residual ultimate strength of metallic pipes under bending moment. Finally, this paper ends with some concluding remarks.

2. Tests overview

In this section, the set-up of four-point bending tests and used specimens are briefly reviewed. The details of the pipe test have been presented in the experimental investigation part [1].

For determining the bending capacity of damaged pipes, a four-point bending test has been conducted, as shown in Fig. 1. The overall length of specimens is 2200 mm with a length of 800 mm under pure bending. The D/t ratio of specimens varied from 20.41 to 23.75 due to manufacturing deviation. The deployed specimen material is Q345B [22], which is a typical material for transmission pipes with the minimum yield strength of 345 MPa. The structural damage, as shown in Fig. 2, is introduced properly by machining method on the specimen before strength test, locating at the center of specimen either on its compression side or on its tensile side. Test results are measured and documented extensively.

The specimens that will be deployed for following comparison with numerical simulations are categorized into two groups (all the series numbers of specimens in this paper are exactly the same with the ones in the experimental investigation): (a) specimen within the first group without artificial structural damage (S1N4); (b) specimens within the third group with metal loss (S3N3 and S3N4).

3. Finite element models

The numerical models have been developed in ABAQUS/Standard [23] through python for the simulation of test specimens and the investigation of parameters' effects, as seen in Fig. 3. An elastic-plastic material with Von Mises yield criterion and isotropic hardening is deployed. The material properties from the material tensile test of the authors [1] are used. This material sample is cut from the longitudinal direction of specimen, with a yield strength of 378 MPa and an ultimate tensile strength of 542 MPa. The detailed stress-strain relationship curve is presented in the experimental part [1]. Therefore, such curves are not listed here for clarity reason. A three dimensional element C3D8R is used for the sake of metal loss damage. The initial imperfection in terms of a wave-type is introduced for all models in the form of eigenvalue buckling mode. The imperfection amplitude is set to $3\%t$ (t is pipe thickness) based on the recommendation from Es et al. [11] due to the lack of data in current test, as seen in Fig. 4.

The model of specimen with metal loss is developed on the basis of test set-up, accounting for the variation of notch size and angle. However, it should be noted that a simplified model has been deployed, removing the contact between specimen and strips for the sake of simulation efficiency. Instead, a simplify-supported boundary condition has been used and two referential nodes have been introduced to represent the loading location of specimen in test, exerting an equivalent forced-rotation through the reference points. It is admitted that discrepancy would be introduced by such a simplification. As described in the experimental part [1], the local deformation in loading places is small enough due to the reinforcement from half-sleeve. Therefore, such effect is minor by using the simplified boundary. In addition, numerical comparisons between full test model and simplified model demonstrate that there is only a small discrepancy for strength prediction, 1% for ultimate bending moment and less than 7% for critical curvature. Detailed comparison results are not presented in this paper for clarity reason. However, these results are going to be published soon.

The shape of notch is based on the physical test with the notch depth (d_m) in the central pipe cross-section. The notch length (l_m) is the chord length of the remaining sector in the pipe cross-section with notch, as seen in Fig. 5. There is a practical reason for this definition. In general, the on-site measurement of straight line is much easier and more accuracy than the measurement of arc length after occurrence of damage. A notch is considered as 90° when its length is along the pipe hoop direction, while a notch is 0° when its length is along the pipe longitudinal direction. The mesh is largely refined around damaged region, with the minimum mesh size equal to 0.8 mm, i.e. less than 1.3% of one half-wave length ($\lambda_{cl} = 1.728\sqrt{Rt}$ [24]) of cylindrical shells. At least four layers of element in thickness direction are deployed to guarantee simulation accuracy.

4. Simulation of experiments

In this section, the structural behavior of specimens in experiments are simulated through the numerical models in previous section. Simulation results have been compared with test data in terms of structural failure modes, bending moment-curvature

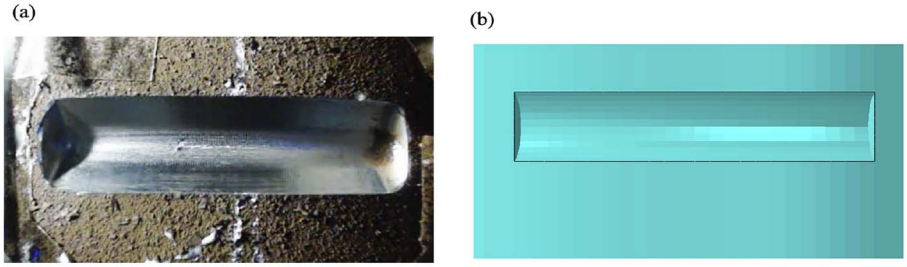

Fig. 2. The notch damage in both test and numerical model: (a) artificial metal loss damage on specimen; (b) metal loss damage on numerical model.

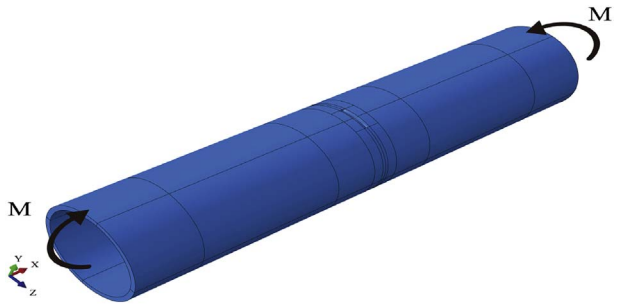

Fig. 3. Simplified numerical model of pipe with metal loss.

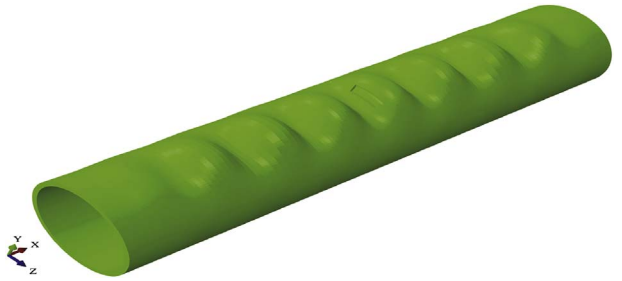

Fig. 4. The initial imperfection in terms of wave-type on pipe surface (imperfection amplitude has been zooming out for the sake of clarity).

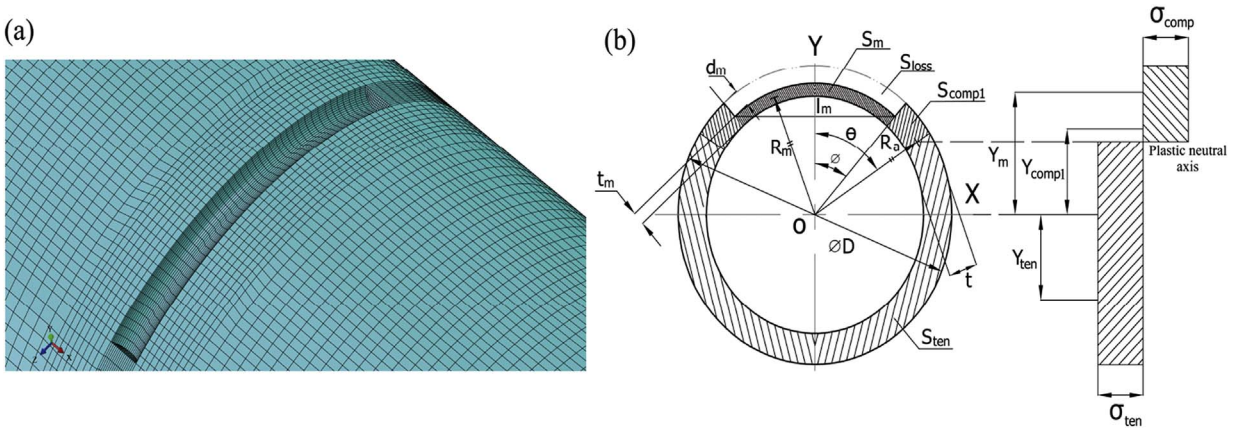

Fig. 5. (a) schema of mesh distribution of notched region; (b) sketch of pipe cross-section with notch and notch parameters.

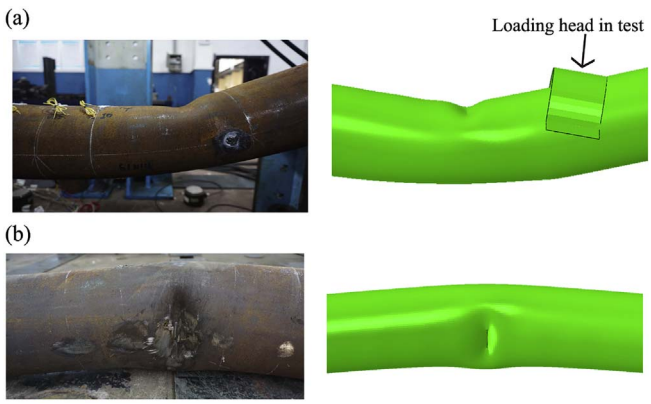

Fig. 6. Representative failure mode of specimens: (a) specimen without damage (S1N4); (b) specimen with metal loss on its compression side (S3N3).

diagrams, and strength capacity.

4.1. Reference values

For comparison of test results in this section, bending moment is normalized by plastic bending moment $M_y = 4R_a^2 t\sigma_y$, while curvature κ is normalized by the curvature-like expression $\kappa_0 = t/4R_a^2$. It should be noted that only global curvature is selected for comparison between test and numerical simulation. The selected locations for calculation of global curvature in simulation are exactly the same with tests. Bending moment in simulation is the resultant of all node forces multiplying their corresponding force arms in the central cross-section of specimen.

4.2. Structural failure modes

The comparison results of structural failure modes of specimens between the numerical prediction and test are illustrated in Fig. 6. Normally, as a result of the increase of structural deformation in the form of ovalization in pipe cross-sections, specimens fail due to the increasing of bending moment. Under a certain extent, such ovalization can be counterbalanced by material yielding and further material hardening so that the structure stays stable. When ovalization cannot be compensated for, the structure reaches its bending capacity with the largest ovalization in a specific pipe cross-section. For instance, the initiation of failure for intact specimen happens on the place far from the center of the specimen, as shown in Fig. 6 (a), whereas the damaged specimen fails in the center of specimen due to the occurrence of damage, as seen in Fig. 6 (b). Both failure mode and location have a good agreement with each other.

4.3. Moment-curvature diagrams

The comparison of bending moment-curvature diagrams between test and numerical predictions is presented in Fig. 7. Specimen S3N3 has a notch with 90^o on its pipe compression side, while specimen S3N4 has a notch with 90^o on its tensile side. The occurrence of notch on the compression side of specimen has changed the variation tendency of bending moment-curvature diagrams, initiating a rapid failure of specimen and considerably reducing the critical bending curvature.

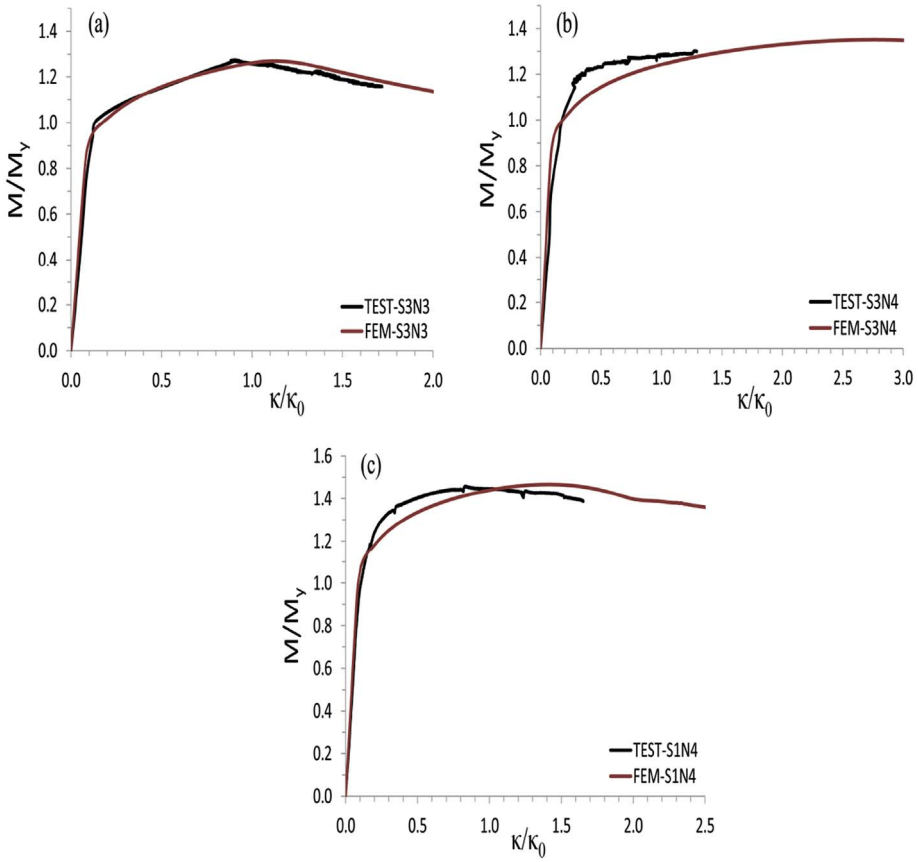

Fig. 7. Comparison between numerical and test results in terms of bending moment-curvature diagram: (a) specimen S3N3 with 90^0 notch on its compression side; (b) specimen S3N4 with 90^0 notch on its tensile side; (c) specimen S1N4 without damage.

Tables 1 and 2 list all comparison results in terms of bending capacity (M_{cr}) and critical curvature (κ_{cr}). For the sake of clarity, results of intact are also presented for comparison. For the prediction result of M_{cr}, less than 2.7% discrepancy has been obtained for the intact specimen, while less than 1.0% discrepancy has been observed for the damaged specimen. The discrepancy of κ_{cr} is less than 2.80% for intact specimen, while it is about 13.1% for the damaged specimen S3N3 with notch on the compression side. These scatters may be introduced by factors such as the material properties and the measurement method for curvature. Detailed discussions have been presented in the experimental investigation part [1]. For specimen S3N4 with a notch on its tensile side, however, the prediction value is nearly double compared with test. One major reason is that the fracture failure in reality has not been accounted for in simulation, which is out of the research domain of this paper. Further investigations are still needed to be done for this scenario. As a consequence, only metal loss on the compression side of pipes is further investigated in this paper.

In addition, the failure procedure between simulation and test is similar with each other. Elastic-plastic failure is dominant, with residual ultimate strength M_{cr} exceeding plastic bending moment M_y to some extent. For an intact specimen, M_{cr} is larger than 1.32 times of M_y, while M_{cr} is more than 1.12 times of M_y for the damaged specimen S3N3 based on predictions. For the damaged specimen S3N4 with a notch on its tensile side, its structure fails in a more smooth way as long as no fracture initiates.

5. Simulation results of metal loss and proposed formulas

In this section, a series of numerical simulations are conducted based on the validated model, changing the geometrical size of notch parameters. The principal dimension of pipes for investigation is listed in Table 3. The simulation results in terms of residual ultimate strength (M_{cr}) and critical curvature (κ_{cr}) are presented in Tables 4–6, where the reference values of M_i and κ_i are described in Section 5.1. In these tables, the notch depth (d_m) is normalized by pipe thickness t, while l_m and w_m are normalized by $\sqrt{Rt}$, expressed as $\lambda_l = l_m/\sqrt{Rt}$ and $\lambda_w = w_m/\sqrt{Rt}$, respectively.

Practically, two criteria are used for the selection of notch size. On the one hand, tiny notch defects may produce stress concentration and undermine the fatigue life under cyclic loading in long term, which is out of the research domain of this paper. On the other hand, extra large notch would introduce a rapid failure of structures in short time, which is also impractical to account for. Therefore, in this paper, the selected notch depth (d_m/t) is between 0.2 and 0.65 ($65\%t$), while the selected notch length (λ_l) is between 0.2 and 4.8 ($\sim 74\%D$). The selected notch width (λ_w) is between 0.3 and 1.4 ($\sim 22\%D$).

5.1. Reference values

In order to have a meaningful comparison of damage effects, the strength value M_i and κ_i from intact pipes are also used as references in the following sections. Reference values M_i and κ_i for numerical results are 101.41 kNm and 0.624 1/m, respectively, obtained through the simulation of intact pipes subjected to bending moment. Meanwhile, reference values for test data from specimen S3N3 are intact results from specimen S1N4, as shown in Table 1.

5.2. Effect of metal loss parameters

In this section, the effects of metal loss in terms of notch depth (d_m) effect, length (l_m) effect and width (w_m) effect are investigated based on the developed numerical model (wave-type initial imperfection with amplitude of 3%t, central location, compression side, 90^o notch). The material anisotropy has not been taken into account. Due to possible fracture failure for pipe with notch on its tensile side, only a notch on the compression side is considered.

Fig. 8 presents the normalized bending moment-curvature diagrams with the variation of notch parameters. Compared with intact pipes, notch damage has a considerable influence on pipe strength. Residual ultimate strength reaches at much lower critical curvature compared with intact pipe. The damaged structures fail rapidly with a fast losing of strength in post-buckling stage.

The effect of each specific parameter of a notch can be clearly seen in Fig. 9. It presents the varying tendency of strength capacity with the changing of different notch parameters. The numerical results indicate that both notch depth and notch length in pipe hoop direction have significant effects on ultimate strength. The larger the d_m or l_m is, the less the bending capacity will be. For instance, a notch depth equal to half of the pipe thickness can reduce M_{cr} and κ_{cr} by more than 54% ad 11%, respectively. In addition, a notch length equal to 2 times of $\sqrt{Rt}$ has reduced M_{cr} and κ_{cr} by nearly 10% and 54%, respectively. The increase of the notch width slightly reduces the pipe strength, presenting a linear tendency, as shown in Figs. 8 (c) and 9 (c). It is also observed that the range of reduction ratio is less than 2% for κ_{cr} and less than 5% for M_{cr} when λ_w increases from 0.4 to 1.4.

5.3. Analytical solution

Providing the bending stress in the entire pipe cross-section is uniform, the compression stress σ_{comp} and the tensile stress σ_{ten} are

Table 1
The results on intact specimen (Dimension unit: mm).

S.N.	D	t	D/t	M_{cr} (Test) (kNm)	M_{cr}(FEA) (kNm)	κ_{cr} (Test) (1/m)	κ_{cr}(FEA) (1/m)
S1N4	167.01	7.84	21.30	102.71	100.40	0.401	0.412

Table 2
The results of specimens with metal loss damage (Dimension unit: mm; Notch angle is 90°).

S.N.	D	t	D/t	Notch ($l_m \times w_m \times d_m$)	Location	M_{cr}(Test) (kNm)	M_{cr}(FEA) (kNm)	κ_{cr}(Test) (1/m)	κ_{cr}(FEA) (1/m)
S3N3	166.89	7.90	21.13	45 × 10 × 3	C[a]	92.89	93.04	0.268	0.303
S3N4	168.3	7.90	21.30	45 × 10 × 3	T[b]	100.00	99.29	0.393	0.791

[a] C denotes the compression side of specimen.
[b] T denotes the tensile side of specimen.

Table 3
The principal dimension of pipe model for numerical investigation.

Pipe type	Diameter D(mm)	Thickness t(mm)	Length L_0(mm)	D/t	L_0/D	Material
Seamless	166.89	7.9	800	21.1	4.79	Q345 [22]

Table 4
Residual ultimate strength of pipes with varying of notch length.

Capacity	d_m = 3 mm, w_m = 10 mm $\lambda_l = l_m/\sqrt{Rt}$											
	0.234	0.467	0.545	0.900	1.000	1.300	1.400	1.500	1.600	1.753	1.900	2.100
M_{cr}/M_i	0.999	0.992	0.988	0.969	0.963	0.947	0.942	0.936	0.931	0.921	0.915	0.905
κ_{cr}/κ_i	0.955	0.888	0.851	0.734	0.704	0.628	0.606	0.583	0.559	0.526	0.506	0.465
	2.400	2.600	2.800	3.000	3.200	3.400	3.800	4.000	4.200	4.400	4.600	4.800
M_{cr}/M_i	0.890	0.882	0.873	0.866	0.859	0.859	0.850	0.847	0.844	0.842	0.844	0.846
κ_{cr}/κ_i	0.417	0.393	0.369	0.353	0.337	0.338	0.313	0.303	0.295	0.295	0.295	0.296

Table 5
Residual ultimate strength of pipes with varying of notch depth.

Capacity	l_m = 45 mm, w_m = 10 mm d_m/t											
	0.20	0.23	0.25	0.27	0.28	0.29	0.30	0.32	0.33	0.35	0.38	0.41
M_{cr}/M_i	0.980	0.964	0.964	0.960	0.956	0.952	0.947	0.939	0.939	0.931	0.921	0.915
κ_{cr}/κ_i	0.792	0.747	0.702	0.688	0.665	0.641	0.628	0.594	0.590	0.559	0.526	0.506
	0.43	0.44	0.46	0.48	0.51	0.53	0.56	0.57	0.58	0.59	0.61	0.63
M_{cr}/M_i	0.908	0.903	0.901	0.895	0.889	0.886	0.882	0.879	0.879	0.877	0.876	0.872
κ_{cr}/κ_i	0.494	0.478	0.481	0.466	0.463	0.457	0.460	0.453	0.465	0.465	0.466	0.462

Table 6
Residual ultimate strength of pipes with varying of notch width.

Capacity	d_m = 3 mm, l_m = 45 mm $\lambda_w = w_m/\sqrt{Rt}$											
	0.389	0.467	0.556	0.584	0.701	0.721	0.821	0.925	1.018	1.104	1.184	1.396
M_{cr}/M_i	0.921	0.914	0.913	0.907	0.911	0.909	0.915	0.904	0.901	0.901	0.900	0.903
κ_{cr}/κ_i	0.526	0.509	0.498	0.496	0.502	0.492	0.522	0.478	0.470	0.465	0.471	0.479

therefore equal to $-\sigma_y$ and σ_y, respectively, when ultimate strength has reached. As a result, the analytical solution of ultimate bending moment of pipe without a notch can be easily derived as $M_y = 4R_a^2 t\sigma_y$.

When the metal loss is induced on pipe surface, as seen in Fig. 5 (b), a typical approach is to remove the corresponding area of the metal loss. Here, a simple derivation of residual ultimate bending strength of pipe with metal loss subjected to bending moment is performed. Assumptions of elastic-perfectly plastic material, full plastic in the damaged cross-section and metal loss on the compression side of pipes are also made.

The plastic neutral axis should be first obtained when residual strength has reached. Based on equilibrium condition, the true axial force F (zero for pure bending) can be expressed as:

$$F = S_m\sigma_{comp} + S_{comp1}\sigma_{comp} + S_{ten}\sigma_{ten} \tag{1}$$

where S_m, S_{comp1}, and S_{ten} are compression area of metal loss region, compression area of region without metal loss, and tensile

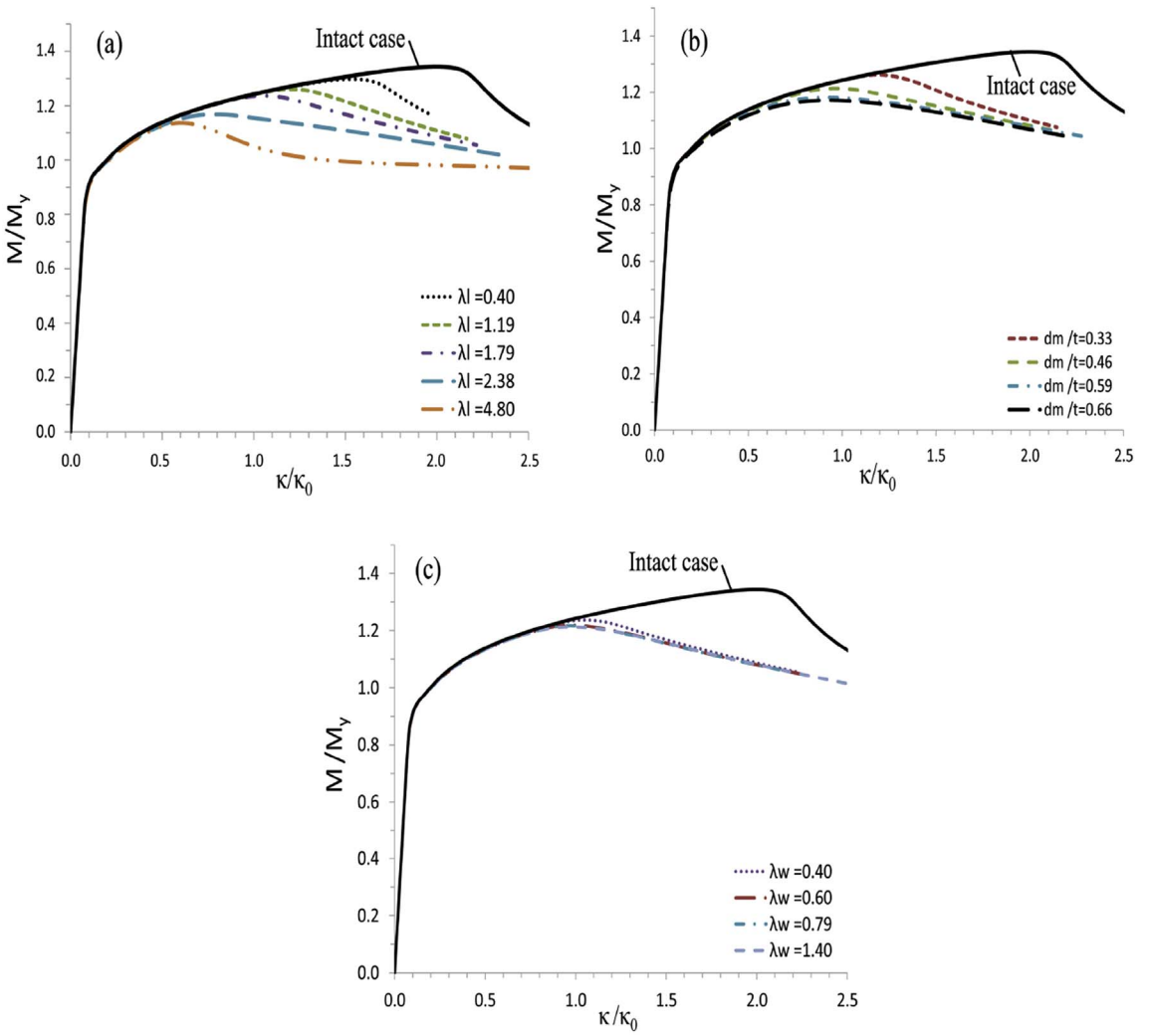

Fig. 8. Normalized bending moment-curvature diagrams with varing of notch parameters: (a) diagrams with variation of normalized notch length (λ_l, w_m = 10 mm, d_m = 3 mm); (b) diagrams with variation of normalized notch depth (d_m/t, l_m = 45 mm, w_m = 10 mm); (c) diagrams with variation of normalized notch width (λ_w, l_m = 45 mm, d_m = 3 mm).

area in pipe cross-section, respectively. They can be expressed as:

$$S_m = 2\int_0^{\phi} R_m t_m d\theta = 2R_m t_m \phi \tag{2}$$

$$S_{comp1} = 2(\theta - \phi)R_a t \tag{3}$$

$$S_{sten} = 2(\pi - \theta)R_a t \tag{4}$$

where $R_m = R_a - \frac{d_m}{2}$ and $t_m = t - d_m$. Substituting Eqs. (2)–(4) into Eq. (1), the angle from bending plane to the plastic neutral axis (θ) can be obtained.

$$\theta = \frac{-F + 2R_a t\sigma_y(\pi + k_1\phi)}{4Rt\sigma_y} = \frac{(\pi + k_1\phi)}{2} \tag{5}$$

$$\phi = arcsin\left(\frac{l_m}{D - 2d_m}\right) \tag{6}$$

where ϕ is the half angle of metal loss (in radians), expressed in Eq. (6), k_1 is a constant related to notch depth, as expressed in Eq. (7). Then we start to derive the residual bending moment (M_{cr}), which can be written as Eq. (8).

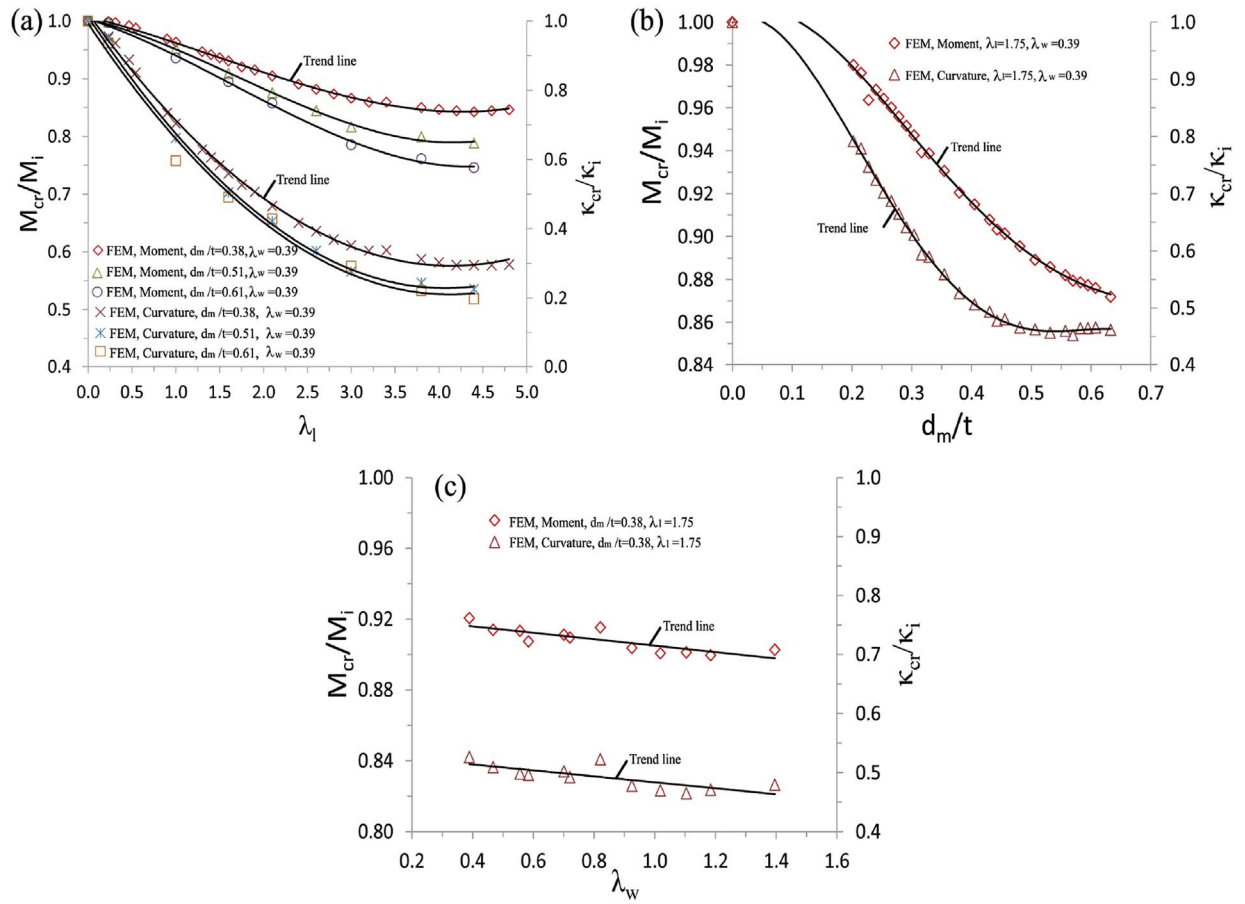

Fig. 9. Variation tendencies of residual bending moment and critical curvature: (a) variation of normalized notch length (λ_l); (b) variation of normalized notch depth (d_m/t); (b) variation of normalized notch width (λ_w).

$$k_1 = 1 - \left(1 - \frac{d_m}{2R_a}\right)\left(1 - \frac{d_m}{t}\right) \tag{7}$$

$$M_{cr} = \sigma_{comp}(S_m Y_m + S_{comp1} Y_{comp1}) + \sigma_{ten} S_{ten} Y_{ten} \tag{8}$$

where Y_m, Y_{comp1}, and Y_{ten} are force arms from bending axis to the mass center of respective area segment. They can be written as:

$$Y_m = \frac{\int_0^{\phi} R_m cos(\theta) \cdot t_m R_m d\theta}{R_m t_m \phi} = \frac{R_a sin(\phi)}{\phi}\left(1 - \frac{d_m}{2R_a}\right) \tag{9}$$

$$Y_{comp1} = R_a \frac{(sin(\theta) - sin(\phi))}{\theta - \phi} \tag{10}$$

$$Y_{ten} = R_a \frac{sin(\theta)}{\pi - \theta} \tag{11}$$

Substituting Eqs. (9)–(11) into Eq. (8), the residual bending moment can be re-written as Eq. (12).

$$M_{cr} = 4R_a^2 t\sigma_y sin(\theta) - 2R_a^2 t\sigma_y k_2 sin(\phi) \tag{12}$$

where k_2 is also a constant related to the depth of metal loss, expressed in Eq. (13). In this equation, the so called "neighbor response" [20] induced by the finite dimension of metal loss (w_m) is not accounted for due to the assumption of infinite metal loss in the pipe longitudinal direction.

$$k_2 = 1 - \left(1 - \frac{d_m}{2R_a}\right)^2\left(1 - \frac{d_m}{t}\right) \tag{13}$$

Hence, the analytical solution for reduction ratio of bending moment is obtained:

$$\frac{M_{cr}}{M_y} = sin(\theta) - \frac{k_2 sin(\phi)}{2} \tag{14}$$

5.4. Proposed formulas

To date, it has been shown from previous research [25] that the loss of notch area dominates the residual ultimate strength of notched structures. Hence, it is reasonable to construct a type of empirical formula including the product of notch length l_m and notch depth d_m. In spite of the minor effect as found in Section 5.2, notch width (w_m) is accounted for to correct the "neighbor response" effect. With these regards, the formulas for both bending moment and critical curvature are constructed as follows:

$$\begin{aligned}\frac{M_{cr}}{M_i}\left(\frac{\kappa_{cr}}{\kappa_i}\right) &= 1 - f\left(\frac{S_{loss}}{S_0}, \lambda_w\right) \\ &= 1 - f(\lambda_l d_m/t, \lambda_w)\end{aligned} \tag{15}$$

where M_i and κ_i are the ultimate bending moment and the critical curvature of intact pipe, respectively. A regression analysis on the FEM results is undertake to build up such relationship.

$$\frac{M_{cr}}{M_i} = 1 - a_1\left(\lambda_l \frac{d_m}{t}\right)^{b_1}(\lambda_w)^{c_1} \tag{16}$$

$$\frac{\kappa_{cr}}{\kappa_i} = 1 - a_2\left(\lambda_l \frac{d_m}{t}\right)^{b_2}(\lambda_w)^{c_2} \tag{17}$$

where a_1, b_1 and c_1 are 0.139, 0.91 and 0.253, respectively; a_2, b_2 and c_2 are 0.652, 0.557 and 0.205, respectively. The prediction results are compared with the test, analytical and simulation results, as shown in Fig. 10. A satisfying comparison has been presented. Compared with the analytical solution, the formula of bending moment produces a lower prediction due to the accounting of notch width effect.

Likewise, the definition from Bai [10] has been used to determine model uncertainty.

$$X = X_{true}/X_{predict} \tag{18}$$

where X_{true} is the data from either experimental test or numerical simulation, and $X_{predict}$ is the prediction values due to proposed equations. It is also assumed that both X_{true} and $X_{predict}$ are from the same cases with the same material properties and geometry. Hence, the mean value (bias), standard error of X, and coefficient of variation (COV) are statistically calculated, as shown in Table 7. The comparison with test has not been conducted since only one valid test data from specimen is available.

It shows that the extent of variability for the prediction of M_{cr} is smaller than 1.5% in relation to the mean bias value. A relative large COV (22.42%) for the prediction of κ_{cr} is obtained. However, a conservative prediction is provided for most of the cases with k_{cr}/k_i between 0.2 and 0.7.

Fig. 11 shows the prediction results of notched metallic pipes with the changing of the loss area of metal loss. Notch width is fixed to 0.39 for all the compared cases. The FEM results are also presented in this figure. With the increase of loss area, both bending moment and curvature decrease considerably. Analysis of variance (ANOVA) shows that R square of the fitted equations are 0.958 and 0.927, respectively, which reflects a high precision of prediction.

In practice, the proposed equations can be used to predict the residual ultimate strength of metallic pipes under dominated bending moment when a scratch in the form of notch is produced due to a sudden mechanical interference such as impact between fishing boat and pipes. A measurement of metal loss length (corresponding chord length), depth and width is needed for estimation. It

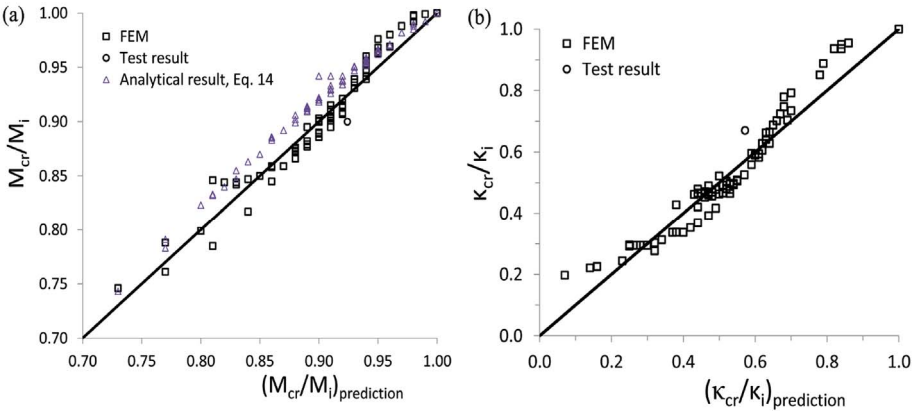

Fig. 10. Comparison among prediction of proposed equations, experimental, numerical results and analytical results: (a) normalized residual ultimate moment (M_{cr}/M_i); (b) normalized critical curvature (κ_{cr}/κ_i).

Table 7
Model uncertainties of the proposed formulas.

X	Moment, Eq. (16)		Curvature, Eq. (17)	
	Mean (Bias)	COV	Mean (Bias)	COV
FEM	1.0012	0.013	1.024	0.2242

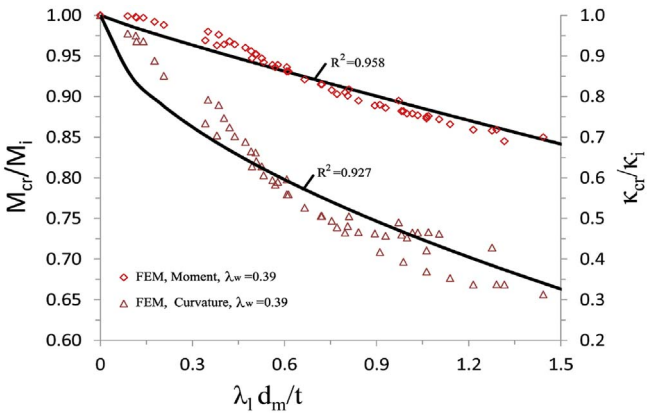

Fig. 11. Prediction of damaged metallic pipes with changing of the loss area of a notch in the damaged pipe cross-section.

should be noted that impact induced residual stress from mechanical interference has not been accounted for in the proposed formulas.

6. Conclusions

On the basis of an experimental investigation, this paper has provided an extensive numerical investigation on seamless pipes with low diameter-to-thickness ratio that suffered from metal loss damage. A simplified numerical model accounting for structural damage has been developed, which can provide a fast modeling tool based on nonlinear FEM. The results of physical test from representative specimens have been numerically simulated and used for validation. Through the numerical models, an investigation of notch parameters has been conducted. The conclusions of this paper are as follows:

1. The developed numerical model is capable of providing an accurate prediction on bending behavior in terms of bending moment, critical curvature and failure mode. Sufficient confidence has been built to deploy these numerical models for residual strength prediction of notched pipes.
2. The occurrence of notch damage on the compression side accelerates the failure of pipe due to the rapid localization of damaged region with an elastic-plastic failure mode.
3. The larger the notch depth (d_m) or the notch length (l_m) is, the smaller the bending capacity will be. The increase of notch width (w_m) slightly reduces pipe strength, presenting a linear tendency.
4. Based on the FEM results, empirical formulas are proposed to predict the residua ultimate strength of metallic pipes under pure bending moment, expressed as a function of loss area of notch in terms of the production of notch depth and length. The effect of notch width is also accounted for in order to correct “neighbor response” effect. These formulas could be utilized for practice purposes to estimate the residual ultimate strength of damaged pipes with metal loss on their compression side, and then facilitate the decision-making of pipe maintenance after mechanical interference. It should be noted that the proposed formulas in this paper are only based on a certain type of metallic pipes with D/t around 21. Further validation is still needed to be done for their applicability in other relevant domains.

Acknowledgments

Thanks to the financial support of China Scholarship Council [grant number 201406 230001]. The funding for the tests that was provided from Section of Transport Engineering and Logistics, Department of Maritime and Transport Technology, Delft University of Technology, the Netherlands, and School of Transportation in Wuhan University of Technology, PR China, is also appreciated.

References

[1] Cai J, Jiang X, Lodewijks G, Pei Z, Zhu L. Experimental investigation of residual ultimate strength of damaged metallic pipelines. ASME 2017 36th international

conference on offshore mechanics and arctic engineering. American Society of Mechanical Engineers; 2017.
[2] Cai J, Jiang X, Lodewijks G. Residual ultimate strength of offshore metallic pipelines with structural damage–a literature review. Ships Offshore Struct 2017:1–19.
[3] DNV. DNV-RP-F101 Corroded pipelines. Det Norske Veritas; 2010.
[4] Mohd MH, Lee BJ, Cui Y, Paik JK. Residual strength of corroded subsea pipelines subject to combined internal pressure and bending moment. Ships Offshore Struct 2015;10(5):554–64.
[5] Lee GH, Seo JK, Paik JK. Condition assessment of damaged elbow in subsea pipelines. Ships Offshore Struct 2017;12(1):135–51.
[6] SreekantaDas H Ghaednia, RichardKania R Wang. Safe burst strength of a pipeline with dent–crack defect: effect of crack depth and operating pressure. Eng Fail Anal 2015;55:288–99.
[7] Bjørnøy O, Rengård O, Fredheim S, Bruce P. Residual strength of dented pipelines, DNV test results. The tenth international offshore and polar engineering conference. International Society of Offshore and Polar Engineers; 2000.
[8] Macdonald K, Cosham A. Best practice for the assessment of defects in pipelines–gouges and dents. Eng Fail Anal 2005;12(5):720–45.
[9] DNV. DNV-RP-F111:Interference between trawl gear and pipelines. latest ed. Det Norske Veritas; 2010.
[10] Bai Y, Igland RT, Moan T. Ultimate limit states of pipes under tension and bending. Int J Offshore Polar Eng 1994;4(04).
[11] Es S, Gresnigt A, Vasilikis D, Karamanos S. Ultimate bending capacity of spiral–welded steel tubes–part i: Experiments. Thin-Walled Struct 2016;102:286–304.
[12] Vasilikis D, Karamanos SA, van Es SH, Gresnigt AM. Ultimate bending capacity of spiral-welded steel tubes–part ii: Predictions. Thin-Walled Struct 2016;102:305–19.
[13] Gresnigt A, Van Foeken R. Local buckling of UOE and seamless steel pipes. The eleventh international offshore and polar engineering conference. International Society of Offshore and Polar Engineers; 2001.
[14] Vitali L, Bartolini L, Askheim D, Peek R, Levold E. Hotpipe JI project: experimental test and FE analyses. ASME 2005 24th international conference on offshore mechanics and arctic engineering. American Society of Mechanical Engineers; 2005. p. 715–29.
[15] Guarracino F, Walker A, Giordano A. Effects of boundary conditions on testing of pipes and finite element modelling. Int J Press Vessels Pip 2009;86(2):196–206.
[16] Hilberink A. Mechanical behaviour of lined pipe PhD Thesis Delft University of Technology; 2011
[17] Bai Q, Bai Y. Subsea pipeline design, analysis, and installation. Gulf Professional Publishing; 2014.
[18] Bai Y, Bai Q. Subsea pipeline integrity and risk management. Gulf Professional Publishing; 2014.
[19] Levold E, Marchionni L, Vitali L, Molinari C, Restelli A, Ozkan IF. Strength and deformation capacity of corroded pipe-laboratory tests and FEM analyses. The twenty-third international offshore and polar engineering conference. International Society of Offshore and Polar Engineers; 2013.
[20] Zheng M, Li J, XX S. Modified expression for predicting the bending resistance of a locally corroded pipeline and its experimental verification. Metals Mater Int 2005;11:215–9.
[21] Park T, Kyriakides S. On the collapse of dented cylinders under external pressure. Int J Mech Sci 1996;38(5):557–78.
[22] GB/T 1591. High strength low alloy structural steels (in Chinese). latest ed. The Chinese National Standard; 2008.
[23] Abaqus6.13. Abaqus: user's manual, 6.13. 2013.
[24] Prabu B, Raviprakash A, Venkatraman A. Parametric study on buckling behaviour of dented short carbon steel cylindrical shell subjected to uniform axial compression. Thin-Walled Struct 2010;48(8):639–49.
[25] Jiang X, Soares CG. Ultimate capacity of rectangular plates with partial depth pits under uniaxial loads. Mar Struct 2012;26(1):27–41.